Applied Catalysis B: Environmental 84 (2008) 659–666

Contents lists available at ScienceDirect

Applied Catalysis B: Environmental

journal homepage: www.elsevier.com/locate/apcatb

Review

Performance of sol–gel Titanium Mixed Metal Oxide electrodes for electro-catalytic oxidation of phenol

M.E. Makgae, M.J. Klink, A.M. Crouch *

Department of Chemistry, Stellenbosch University, Private Bag X1, Matieland 7602, South Africa

ARTICLE INFO

Article history:
Received 3 March 2008
Received in revised form 16 May 2008
Accepted 23 May 2008
Available online 21 July 2008

Keywords:
Electro-catalysis
Mixed metal oxide electrodes
Phenol oxidation

ABSTRACT

Mixed metal oxides SnO_2–RuO_2–IrO_2, Ta_2O_5–IrO_2 and RhO_2–IrO_2 were immobilised on a Ti substrate using sol–gel techniques. The Ti mixed metal oxides were characterized in terms of morphology using scanning electron microscopy. Cyclic voltammetric responses of phenol at Ti/SnO_2–RuO_2–IrO_2, Ti/Ta_2O_5–IrO_2 and Ti/RhO_2–IrO_2 electrodes were evaluated and showed significantly low potentials for Ti/Ta_2O_5–IrO_2 (+100 mV), Ti/SnO_2–RuO_2–IrO_2 (+200 mV) and Ti/RhO_2–IrO_2 (−100 mV). The degradation of phenol in aqueous solution and its intermediates were investigated by bulk electrolysis and quantitatively assessed by HPLC analysis to elucidate the decomposition pathways and to develop a kinetic model for the electro-catalytic oxidation of phenol over Ti mixed metal oxides. Ring compounds, benzoquinone/hydroquinone, catechol, and short chain organics, carboxylic acids, have been identified as intermediate products for the electro-catalytic oxidation of phenol. Fundamental kinetic data were obtained for the conversion of phenol at these electrodes and was found to proceed in accordance with the pseudo-first-order kinetics with respect to the phenol concentration.

Contents

1. Introduction

Widespread contamination of water by phenol has been recognized as an issue of growing importance in recent years. It has attracted more attention for research because of its toxicity

* Corresponding author. Tel.: +27 21 808 3535; fax: +27 21 808 3342.
E-mail address: amc@sun.ac.za (A.M. Crouch).

0926-3373/$ – see front matter © 2008 Elsevier B.V. All rights reserved.
doi:10.1016/j.apcatb.2008.05.021

and the frequency of industrial processes producing waters contaminated by phenol [1–4]. Phenol is carcinogenic and is a considerable health concern, even at low concentration. The main sources of phenolic wastewater are industries such as petrochemicals, coal gasification, pesticides manufacture, electroplating and metallurgical operations [5–8]. In addition, phenol is considered to be an intermediate product in the oxidation pathway of higher molecular weight aromatic hydrocarbons, thus it is often used as a model compound for advanced wastewater treatments [1,3,5].

Many technologies have been investigated for removing and degradation of phenolic compounds in wastewater. They include photocatalytic oxidation [5], wet oxidation [6], supercritical water oxidation [8], adsorption [9] and biological treatment [10]. Several researchers [1,3,4,11–15] have worked on the electrochemical destruction of phenolic wastes, but to date it has not been considered to be commercially viable because of a low phenol reaction rate and/or low removal and destruction efficiency.

Thus far, oxidation technology has shown its potential to destroy phenol completely in wastewater. Although this process (phenol oxidation) was demonstrated before [14–24], there is still considerable controversy about the reaction mechanism of this anodic oxidation process [25]. The mechanism of electrochemical oxidation of phenol has been studied by various researchers [1,3,6,11,13,20,25]. It is generally considered that phenol oxidation starts with a one electron transfer, leading to a phenoxy radical reaction. It is further considered that some possible reactions of phenoxy radical relate to radial–radial coupling, radial disproportionation, radial elimination or radial oxidation to cation, and then followed by benzoquinone formation [18,26–31]. It is possible that intermediate species in aqueous phenol solution are formed before the detection of benzoquinone and are not detected because of their instability.

Most researchers believe that benzoquinone/hydroquinone is an important intermediate, and that the benzoquinone degrades to form various carboxylic acids [22,23,32,33]. Different researchers have proposed the formation of various carboxylic acids under various experimental conditions [1,18,23,33]. The process of carboxylic acid degradation was more complicated than benzoquinone formation. There are several suggested mechanisms for benzoquinone degradation. If benzoquinone is absorbed onto the electrode surface and gives an electron, an adsorbed OH radical will attack the benzoquinone. When this process repeats itself at the para position, the aromatic ring could be opened, resulting in the formation of malic or maleic acid and other small organic acids, such as oxalic and malonic acids.

Phenol has been oxidized at electrodes such as graphite [16], platinum [17], bismuth-doped lead dioxide [18] and SnO_2–Sb_2O_5 [14]. The encountered problems of electrode fouling, which reduces the efficiency of the process and hinders it from practical implementation has been a draw-back [14,19].

Furthermore, the development of non-toxic anode materials, as well as anodes exhibiting good efficiencies for the oxidation of organic compounds down to low concentration, is needed. Currently, promising materials are doped tin oxide and doped lead oxide as thin films on titanium, which seem to allow complete oxidation of many organics [14,26]. They are however, prone to fouling due to the intermediate degradation products. Stability of these electrodes over a long period also has not been proven conclusively.

In this work the measure of the effect of different mixed metal oxides on a Ti substrate towards the oxidation of phenol were studied under neutral, alkaline and acidic conditions. The effects of pH on the phenol decomposition, intermediates and kinetics will also be investigated.

2. Experimental

2.1. Reagents

Reagents $TaCl_5$, $RuCl_3$, $SnCl_2$, $RhCl_3$, $IrCl_3$, Na_2HPO_4, Ti foil and C_6H_5OH were obtained from Aldrich (Germany). Merck's absolute ethanol, methanol, potassium chloride and hydrochloric acid were used in the experiments. All reagents were of analytical grade, were used without further purification and were purchased in Cape Town (South Africa).

2.2. Sol–gel and thin film preparation

The metal oxides were prepared by dissolving hydrated chloride precursors in absolute ethanol using a sol–gel technique. The sol–gel synthesis for the metal oxides titanium materials were based on synthesis procedures modified from literature [27,28]. The starting materials were placed in a round-bottomed flask fitted with a thermometer, and the solutions were well stirred and refluxed for 1 h, before being left to age at room temperature for at least 24 h to ensure ageing of the gel. For the purpose of producing the thin films, the gels were retained in the liquid form. The titanium substrates were cut to size (1 cm × 1 cm), sandblasted and etched in HCl (11.5 M) for 5 min, rinsed with copious amounts of UHQ water and finally rinsed with absolute ethanol and dried with air.

The Ti substrates were dipped into the gel solution and then slowly withdrawn at a rate of 80 mm min^{-1}. The titanium substrates onto which thin metal oxides films were coated were affixed to the rotating disk surface and rotated at full speed (∼1000 rpm) for 10 s to give reproducible thin films. The thin films were then annealed in an oxygen-rich atmosphere in a quartz tube furnace at a slow heating rate (1 °C/min) up to 700 °C and then allowed to cool to room temperature, under ambient conditions.

2.3. Electrodes preparation

The electrical connection was made through a Cu wire welded to the metal oxides titanium substrate by means of silver epoxy. The back of the electrode and the copper contact was isolated with an inert-conductive polymer resin to base the results exclusively on the active surface. The composition ratio of the conducting metal oxides was varied to investigate the electro-catalytic activity using cyclic voltammetry (CV).

3. Analytical methods

3.1. Scanning electron microscopy (SEM)

The surface morphologies of the electrodes were analyzed by SEM. An ABT60 Scanning Electron Microscope was used for the experiments. The SEM pictures were taken at a working distance of 7 mm and an accelerating voltage of 7 kV. The samples were placed horizontally on the stubs and they were not coated for viewing. For the X-ray analysis, the working distance was 12 mm and the accelerating voltage was 25 kV. The samples were tilted at 30°. The SEM cross-sections of the thin films were obtain as follows: the samples were left in a resin for 24 h in an oven at 60 °C, cut and polished into small pieces and mounted vertically on the stubs.

3.2. Electrochemical measurements

The surfaces of the modified electrodes were characterized by means of cyclic voltammetric curves to evaluate the catalytic response of the electrode surfaces. All electrochemical experi-

ments were carried out and recorded on a BAS 50/W electrochemical analyzer (Bioanalytical Systems, Lafayette, IN, USA). The electrolysis of phenol (0.05 mM) solution was carried out in a 0.01 M KCl medium. The geometric area of the working electrode was 1 cm^2. The cell (50 ml) was degassed with nitrogen for 20 min to exclude any oxygen from the solution. A conventional three electrode system was employed: the working electrodes were composites of Ti/SnO_2–RuO_2–IrO_2, Ti/Ta_2O_5–IrO_2 and Ti/RhO_2–IrO_2, respectively. Silver/silver chloride (Ag/AgCl) and a platinum wire were used as reference and auxiliary electrodes, respectively. Voltammograms were recorded at 25 °C, anodically at a potential scan rate of 100 mV/s. The pH of the samples was varied (pH 2, 7 and 12) and measured by a Crison pH meter. Bulk electrolysis was carried out at a potential of 1500 mV.

3.3. HPLC analysis

The progress of the electrochemical oxidation of phenol was monitored by HPLC (Waters™). HPLC is characterized by high speed and efficiency, and can be coupled to many sensitive and selective detectors [29]. Compounds produced during the oxidation of phenol belong to a number of different chemical families having widely varying solubilities, polarities and dissociation constants [30]. Two different chromatographic conditions were used for analysis: The first column used for analyzing the aromatic compounds was a Luna 5 μ C18 (2) column with water–methanol (50:50, v/v) as mobile phase under isocratic elution and a flow rate of 1 ml/min for aromatics. The 10 μl samples were injected into the column. Water and methanol were used as a mobile phase and was filtered (<1 μm pores) and degassed. The system was flushed with pure methanol then the column was connected with the correct direction of flow. The column was again flushed with methanol/water (50:50, v/v) for 10–20 min. The UV detector was set at wavelengths between 200 and 400 nm.

The second type of analysis for organic acids made use of a C18 Atlantis column with a mobile phase of Na_2HPO_4 and a flow rate of 1 ml/min. Detection of analytes were with UV detection at a wavelength λ = 210 nm for organic acids. The identification of the indicated intermediate compounds was achieved by comparing migration times of the model mixture of phenol, hydroquinone, benzoquinone and catechol with the samples. The results were reproducible, the day to day precision of retention times were within 0.1 and 1.2% relative standard deviation.

4. Results and discussion

4.1. Scanning electron microscopy

The morphology of the electrode coatings strongly depends on the composition of the precursor solutions and the conditions of preparations. Fig. 1(a) shows the microstructure of the Ti/IrO_2–Ta_2O_5 electrode. The micrograph showed a heterogeneous cracked morphology consisting of flat, smooth areas and agglomerated particles formed on smooth areas. These aggregated particles were attributed to IrO_2 and the flat area to the combination of both tantalum and iridium oxides. Which is in agreement with Roginskaya et al. [31] who reported that the boundaries of IrO_2 crystallites are modified by Ta_2O_5 in mixed oxides and the finer the crystallites of IrO_2, the greater the contribution of Ta_2O_5 modification to the mixed modified phase. Results of the SEM cross-sectional surface area analysis estimated the film thickness to be about 1.9 μm (Fig. 1(b)).

The SEM morphology of the Ti/RhO_x–IrO_2 coating layer (Fig. 2(a)) appeared to be uniformly distributed. A rough coating with a grain-like appearance in the nanometer size was observed

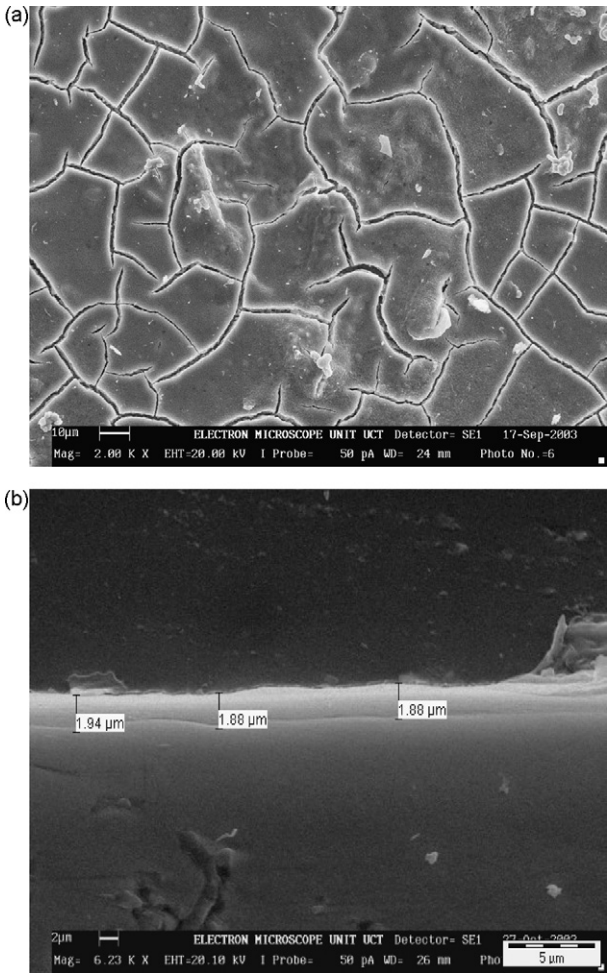

Fig. 1. (a) SEM surface image and (b) SEM cross-sectional surface image of a Ti/Ta_2O_5–IrO_2 electrode.

in the scanning electron micrographs [32]. These grain formations, was a result of Rh increased that exposed the Ti substrate. The exposing of the Ti substrate leads to the formation of a thin film of TiO_2. The thickness of the coating was found to be ~1.62 μm and the side view indicated the formation of a homogeneous film (Fig. 2(b)) [28,32].

Crouch et al. reported on a SEM image and a SEM cross-sectional surface of the Ti/SnO_2–RuO_2–IrO_2 thin films. The SEM micrograph showed a rough morphology with a network structure and a porous-like surface for the oxide coatings. Their pore dimensions range between 1.5 and 2 μm in diameter. They also determined the film thickness from analysis of the SEM cross-sectional surface area and estimated to be about 1.6 μm, which they claimed depends on the rate of dip-coating. Their side view indicates the formation of a homogeneous film [28].

4.2. Cyclic voltammetric measurements

CV was used to evaluate the catalytic response of phenol on the different electrode surfaces and to evaluate the reversibility and kinetics of the electrodes surfaces. Fig. 3 shows the voltammograms of electrodes (a) Ti/Ta_2O_5–IrO_2 without phenol and (b) Ti/Ta_2O_5–IrO_2 with 0.05 mM phenol at a scan rate of 20 mV/s in 0.01 M KCl. According to the cyclic voltammograms the oxygen evolution potential of the Ti/Ta_2O_5–IrO_2 was seen to be lower than the Ti electrode. The voltammogram also shows quasi-reversible

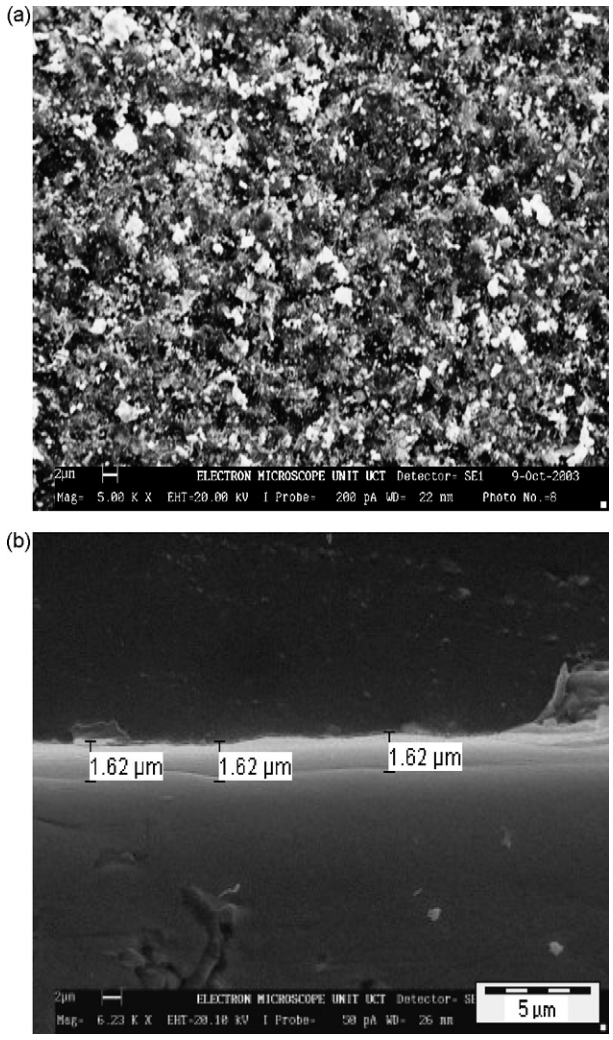

Fig. 2. (a) SEM surface image and (b) SEM cross-sectional surface image of a Ti/RhO_2–IrO_2 electrode.

processes when phenol was added, which confirmed the oxidation/reduction chemistry of phenol at the Ti/Ta_2O_5–IrO_2 electrode. Crouch et al. observed similar behaviour for the oxidation of phenol at Ti/SnO_2–RuO_2–IrO_2 (+200 mV) and Ti/RhO_2–IrO_2 (−100 mV) electrodes, respectively. The oxidation potential of

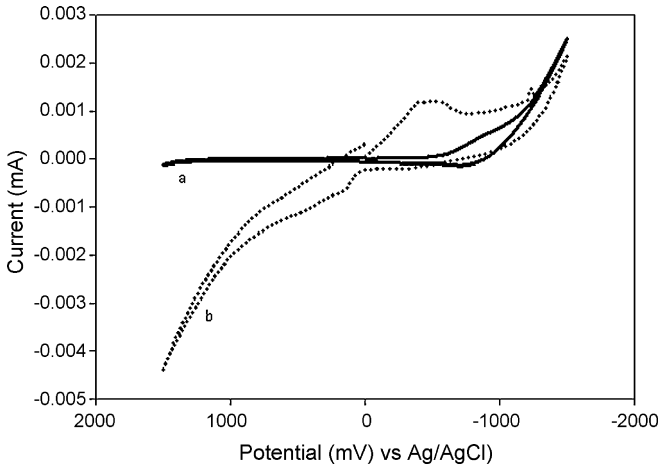

Fig. 3. shows the voltammograms of electrodes (a) Ti/Ta_2O_5–IrO_2 without phenol and (b) Ti/Ta_2O_5–IrO_2 with 0.05 mM phenol at a scan rate of 20 mV/s in 0.01 M KCl.

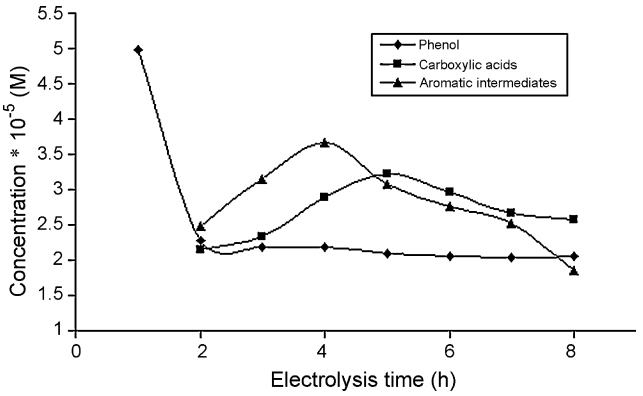

Fig. 4. The breakdown of phenol into its by-products during electrolysis using Ti/SnO_2–RuO_2–IrO_2 electrode system as determined by HPLC and PDA.

the metal oxides were very low (950 mV) compared to when Pt (Ag/AgCl) was used, indicating that the metal oxides significantly lowered the over potential for the oxidation of phenol [28].

4.3. Performance of modified electrodes on phenol degradation

Bulk electrolysis experiments were carried out to monitor the performance of the modified electrodes on the degradation of phenol under batch conditions. The profiles presented serves as a point of reference for comparing the breakdown profiles of phenol on the different electrodes. The total organic carbon (TOC) content and formation of CO_2 were however not measured. An individual presentation of the different aromatic compounds and the carboxylic acids are not presented here, since the rates of degradation of these are different. The concentrations of the aromatics and the carboxylic acids were compounded and only measured after 2 h from the start of the experiment. The phenol removal efficiency was calculated according to the formula:

$$\frac{[\mathrm{Ph}]_\mathrm{T} - [\mathrm{Ph}]_\mathrm{end}}{[\mathrm{Ph}]_\mathrm{T}} \times 100$$

where $[\mathrm{Ph}]_\mathrm{T}$ is the total phenol concentration and $[\mathrm{Ph}]_\mathrm{end}$ the phenol concentration at the end of the reaction. The Ti/SnO_2–

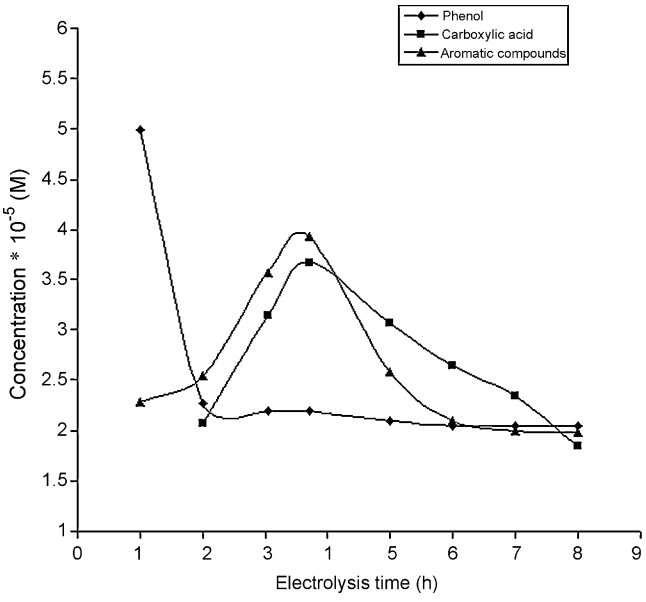

Fig. 5. The breakdown of phenol into its by-products during electrolysis using Ti/Ta_2O_5–IrO_2 electrode system as determined by HPLC and PDA.

RuO_2–IrO_2 electrode system (Fig. 4) showed a rapid degradation of phenol for the first 2 h, after which the aromatic compounds and carboxylic acids were formed. The aromatic compounds concentrations were seen to increase for 2 h and then gradually decrease. The concentration of the carboxylic acids increased and reached the maximum height at 5 h and then decreased with time.

Bulk electrolysis results of phenol using the Ti/Ta_2O_5–IrO_2 electrode system (Fig. 5) showed that the phenol concentration decreases with time after 1 h with the simultaneous formation of aromatic compounds at low concentrations. The conversion of aromatic intermediates to the organic acid intermediates took place much faster. Aromatic intermediates were oxidized to form carboxylic acids in 2 h. Both the aromatic compounds and the carboxylic acids reached their maxima at 4 h, but the concentration of the aromatic compounds decreased drastically afterwards and reached a constant concentration after 6 h.

Oxidation processes on the Ti/RhO_2–IrO_2 electrode system (Fig. 6) showed that as phenol degraded, the aromatic compounds were formed to significant amounts within 2 h. The concentration of the aromatic compounds increased with time and reached a maximum after 5 h with a simultaneous formation of carboxylic acids. The concentration of the carboxylic acids increased and reached a maximum at 7 h then decreased with time. Thus suggest that a different breakdown mechanism for phenol is operative in the case when the Ti/RhO_2–IrO_2 electrode system was used.

The profiles suggest that the Ti/Ta_2O_5–IrO_2 electrode combination of metal oxides is the most efficient of the three electrode surfaces, although phenol removal was achieved by all the modified electrodes. Baker et al., in their results on metal oxide properties, found that the efficiency removal of *p*-benzoquinones are improved using materials that have a low porosity and only a few active sites [32].

4.4. Kinetic study of the titanium mixed metal oxides

The activities of the catalytic systems were evaluated both on the basis of phenol removal efficiency, as well as the rate constants (K/h) determined in accordance with kinetic equations. The results from the kinetic investigation in regard to the liquid/phase electrocatalytic oxidation of phenol with the Ti/SnO_2–RuO_2–IrO_2, Ti/Ta_2O_5–IrO_2 and Ti/RhO_2–IrO_2 electrodes using different pH media are presented in Figs. 7–9. The plots of $\ln(C_0/C)$ as a function of time showed straight lines for all the studied samples. Therefore, it may

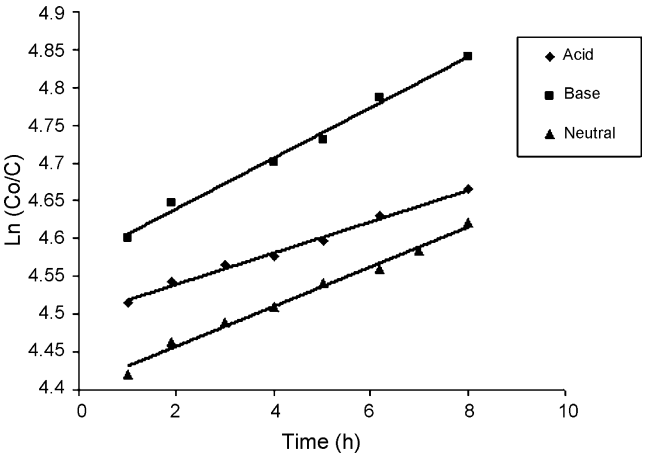

Fig. 7. A plot of $\ln(C_0/C)$ as a function of time using different pH media for the Ti/SnO_2–RuO_2–IrO_2 electrode system, where C is the final and C_0 is the initial concentration.

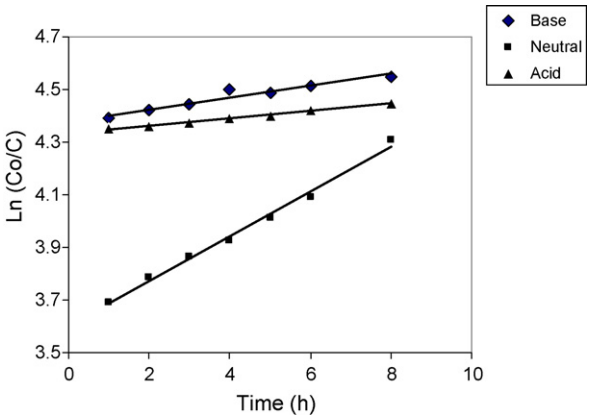

Fig. 8. A plot of $\ln(C_0/C)$ as a function of time using different pH media for Ti/Ta_2O_5–IrO_2 electrode system, where C is the final and C_0 is the initial concentration.

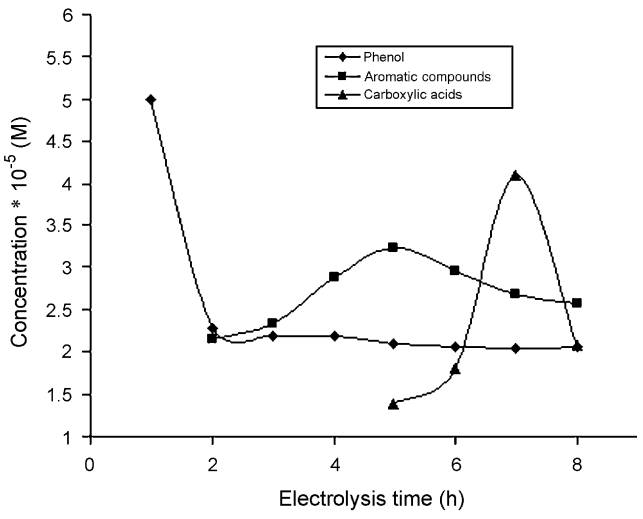

Fig. 6. The breakdown of phenol into its by-products during electrolysis using Ti/RhO_2–IrO_2 system as determined by HPLC and PDA.

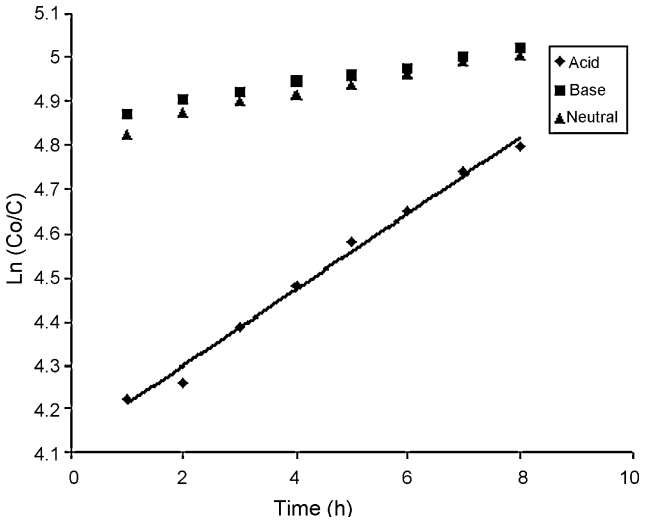

Fig. 9. A plot of $\ln(C_0/C)$ as a function of time using different pH media for the Ti/RhO_2–IrO_2 system, where C is the final and C_0 is the initial concentration.

Table 1
The removal or conversion percentage and rate constants of the phenol oxidation process on the studied surfaces at various pH values

Type of electrodes	pH values	Phenol removal efficiency (%)	Rate constants (K/h)
$Ti/SnO_2–RuO_2–IrO_2$	2	99	0.0101
	7	99	0.0266
	12	99.2	0.0322
$Ti/Ta_2O_5–IrO_2$	2	98.8	0.0145
	7	98.6	0.0856
	12	98.9	0.0226
$Ti/RhO_2–IrO_2$	2	99.1	0.0202
	7	99.1	0.0244
	12	99.3	0.0870

be assumed that the electro-catalytic oxidation of phenol proceeds in accordance with a pseudo-first-order kinetics with respect to the phenol concentration. The slope of all the samples upon linear regression is equal to the first-order rate constant and the estimated values of constants are presented in Table 1. The fact that all the experiments were conducted by continuously bubbling air through the liquid phase, the concentration of oxygen dissolved in the liquid was held constant throughout the duration of the oxidation process. Hence, the rate of the reaction is independent on the oxygen concentration [22,33–47].

The results concerning the effect of pH are summarized in Table 1 and showed that an increased in solution pH enhances the removal efficiency of phenol. The different behaviour observed for basic, neutral and acidic could be attributed to the different reactivities with oxygen of the three forms of phenol found in the liquid, namely phenolate ion, non-protonated and protonated. Highest rates of oxidations were achieved at pH 12, when the pH was set above the dissociation constant of phenol (p*K* 9.95). This is attributed to the fact that at high pH phenol tends to exist as phenolate anions which have high solubility and will not adsorbed significantly [48].

4.5. Proposed pathway of the electrochemical oxidation of phenol at different pH

The experimental results suggest that electro-catalytic phenol oxidation on different metal oxide thin films may follow different reaction pathways (Figs. 7–9). The chromatography results (not shown here) showed that the main aromatic products formed during the oxidation of phenol was benzoquinone, hydroquinone and catechol. HPLC analysis and UV spectra indicated the specific wavelengths where these intermediate compounds were formed. For example: hydroquinone (λ_{max} = 220 and 290 nm), benzoquinone (λ_{max} = 270 nm), catechol (λ_{max} = 290 nm) and phenol (λ_{max} = 254 and 270 nm). The aromatic ring intermediate compounds were formed and subsequently oxidized to form aliphatic carboxylic acids; malic, malonic and oxalic acid.

At basic conditions (Schemes 1a, 2a and 3a) the thin film electrodes seems to follow the same degradation pathway up until the malonic acid intermediate, where the malonic acid is first degraded to acetic acid and then oxalic acid for the $Ti/SnO_2–RuO_2–$

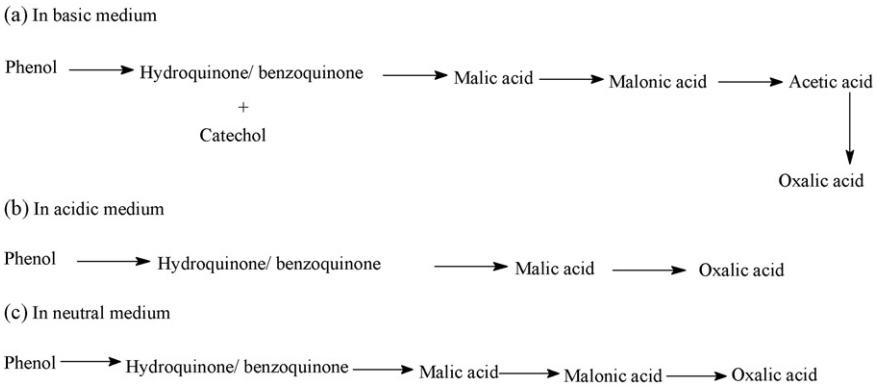

Scheme 1. $Ti/SnO_2–RuO_2–IrO_2$ system.

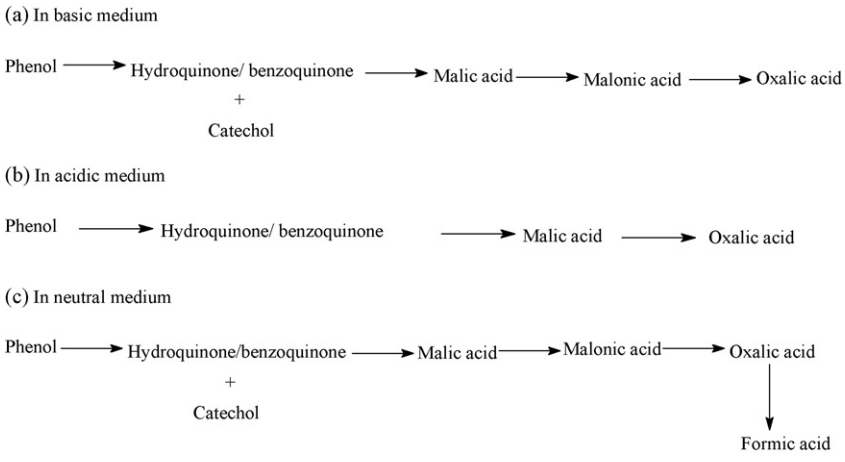

Scheme 2. The $Ti/Ta_2O_5–IrO_2$ system.

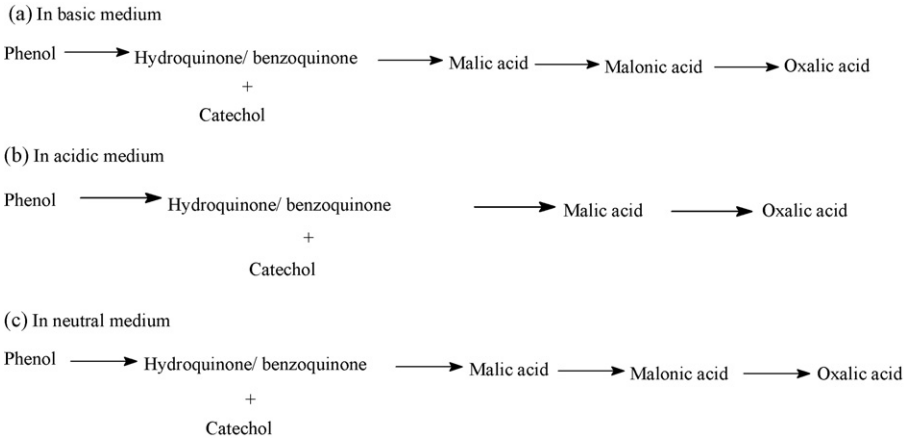

Scheme 3. The Ti/RhO_2–IrO_2 system.

IrO_2 system. The acetic acid comes from the decarboxylation of malonic acid but it has not been found for Ti/Ta_2O_5–IrO_2 and Ti/RhO_2–IrO_2 electrodes probably due to the high carboxylation rate at these electrodes [49].

In acidic media (Schemes 1b, 2b and 3b) similar degradation pathways were also observed as in the basic media, except for the electrode Ti/Ta_2O_5–IrO_2 system catechol was also one of the intermediates.

In neutral media (Schemes 1c, 2c and 3c) the Ti/SnO_2–RuO_2–IrO_2 and the Ti/RhO_2–IrO_2 system electrodes followed similar phenol degradation patterns with oxalic acid as the end product, whereas the Ti/Ta_2O_5–IrO_2 system formed formic acid as its final oxidation product.

As seen from Schemes 1–3, which are in agreement with Duprez et al. [50], all the oxidation routes consider the hydroxylation of phenol to hydroquinone and catechol as a first step. The relationship between the properties of the metal oxide materials and the removal rate of the intermediates [51] also played a significant role as is the pH of the medium [48] when it comes to oxidation pathways of phenol. A proposed reaction pathway for the phenol electro-catalytic oxidation on mixed metal oxides for this work is presented in Fig. 10. Santos et al. reported similar pathways for the oxidation of phenol. They proved that the hydroquinone was oxidized to *p*-benzoquinone, whereas catechol was directly oxidized to oxalic acid and CO_2 [3].

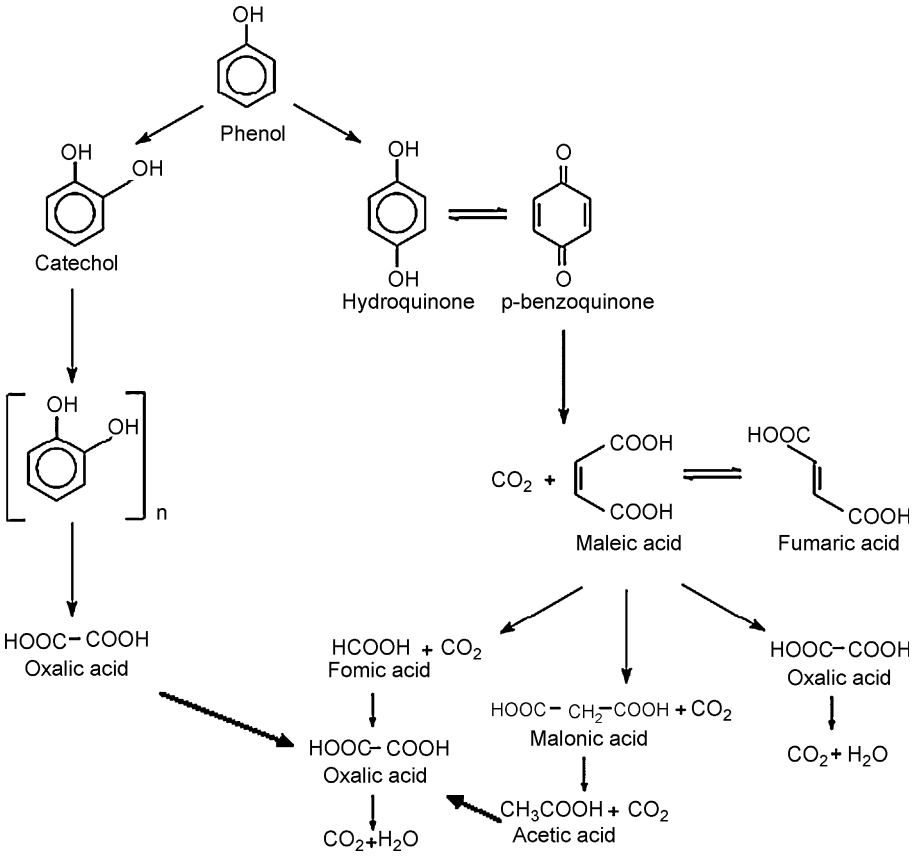

Fig. 10. Reaction pathway for the phenol electro-catalytic oxidation on mixed metal oxides proposed in this work.

5. Conclusions

The mixed metal oxide materials used in this study are good electronic conductors at anode potentials. They also have high surface roughness and some internal porosity, which is equivalent to a large number of electro-active sites; hence, these oxides exhibit a high electro-catalytic activity for the oxygen evolution per geometrical oxide. This is reflected in the results, indicated by the performance of these oxides towards phenol removal efficiency. Hu et al. also found in binary system combination of $IrO_2 + Ta_2O_5$ possess a higher maximum activity and higher stability for the O_2 evolution reaction in acid solution [52]. Similar results were obtained by Baglio et al. when IrO_2–RuO_2 electrocatalyst were used for oxygen evolution reactions [53].

Electrochemical oxidation for treating aqueous phenol solutions was successful using these electrodes. The removal or conversion efficiency of the phenol oxidation was found to be more than 90%. However, the mineralization of phenol is never total, even at high conversion. The pathways of the electrochemical oxidation of phenol, summarized in Schemes 1–3, were proposed for different prepared metal oxide electrodes. HPLC results showed that phenol yielded intermediate ring compounds as hydroquinone, benzoquinone, catechol and carboxylic acids such as malic, malonic, acetic, oxalic and formic. Kinetic studies of phenol on these mixed metal oxide electrodes were also investigated and was found to occur via a quasi-first-order rate. This study serves to confirm further that mixed metal oxide electrodes used as ternary oxides can be effectively tailored to address the thermodynamic and kinetic barriers associated with the oxidation of complex organic molecules.

Acknowledgements

The authors would like to thank the National Research Foundation (NRF) of South Africa for financial assistance. A grant from ESKOM (Tertiary Education Support Programme) is sincerely appreciated.

References

[1] J. Chen, B. Preston, M. Zimmerman, J. Chromatogr. A 781 (1997) 205–213.
[2] A. Idris, K. Saed, Global Nest: The International Journal 4 (2/3) (2002) 139–144.
[3] A. Santos, P. Yustos, A. Quintanilla, S. Rodriguez, F. Garcia-Ochoa, Appl. Catal. B: Environ. 39 (2002) 97–113.
[4] D. He, S. Mho, J. Electroanal. Chem. 568 (2004) 19–27.
[5] M.A. Barakat, J.M. Tseng, C.P. Huang, Appl. Catal. B: Environ. 59 (2005) 99–104.
[6] A. Santos, P. Yustos, A. Quintanilla, F. Garcia-Ochoa, Chem. Eng. Sci. 60 (2005) 4868–4880.
[7] A. Santos, P. Yustos, T. Cordero, S. Gomis, S. Rodriguez, F. Garcia-Ochoa, Catal. Today 101–102 (2005) 213–218.
[8] G. Sudama, P. Savage, AIChE J. 41 (8) (1995) 1864–1873.
[9] S. Rengaraj, S. Moon, R. Sivablan, B. Arabind, V. Murugesan, J. Hazard. Mater. 89 (2002) 185–196.
[10] E. Miland, M. Smyth, C. Fagain, J. Chem. Technol. Biotechnol. 67 (1996) 227–236.
[11] H. Sharifian, D.W. Kirk, J. Electrochem. Soc. 133 (5) (1986) 921–924.
[12] M. Gatrell, B. MacDougall, J. Electrochem. Soc. 146 (9) (1998) 3335–3348.
[13] J.L. Boudenne, O. Cerclier, J. Galea, E. Van der Vlist, Appl. Catal. A: Gen. 143 (2) (1996) 185–202.
[14] J. Grimm, D. Bessarabov, W. Maier, S. Storck, R.D. Sanderson, Desalination 115 (1998) 295–302.
[15] C. Comninellis, G.P. Vercesi, J. Appl. Electrochem. 21 (1991) 335–345.
[16] Y.M. Awad, N.S. Abuzaid, Sep. Purif. Technol. 18 (2000) 227–236.
[17] C. Comninellis, C. Pulgarin, J. Appl. Electrochem. 21 (1991) 703–708.
[18] N.B. Tahar, A. Savall, J. Appl. Electrochem. 29 (1999) 277–283.
[19] C. Comninellis, Electrochim. Acta 39 (11–12) (1994) 1857–1862.
[20] J. Chen, L. Eberlein, C. Langford, J. Photochem. Photobiol. A: Chem. 148 (2002) 183–189.
[21] Y.M. Awad, N.S. Abuzaid, Sep. Sci. Technol. 34 (4) (1999) 699–708.
[22] M.O. Azzam, Y. Tahboub, M. Altarazi, Trans. IChem B 77 (1999) 219–226.
[23] M.O. Azzam, Y. Tahboub, M. Altarazi, J. Hazard. Mater. B 75 (2000) 99–113.
[24] S. Trasatti, Electrochim. Acta 45 (15–16) (2000) 2377–2385.
[25] C. Bock, B. MacDougall, Electrochim. Acta 47 (2002) 3361–3373.
[26] B. Correa-Lozano, C. Comninellis, A. De Basttisti, J. Electrochem. Soc. 143 (1) (1996) 203–209.
[27] L. Lipp, D. Pletcher, Electrochim. Acta 42 (7) (1997) 1101–1111.
[28] M. Makgae, C. Theron, W. Przybylowicz, A. Crouch, Mater. Chem. Phys. 92 (2005) 559–564.
[29] H.Z. Lian, L. Mao, X.L. Ye, J. Miao, J. Pharm. Biomed. Anal. 19 (1999) 621–625.
[30] Y. Fiamegos, C. Stalikas, G. Pilidis, Anal. Chim. Acta 467 (1–2) (2002) 105–114.
[31] Y.E. Roginskaya, O.V. Morozova, G.I. Kaplan, R.R. Shifrina, M. Smirnov, S. Trasatti, Electrochim. Acta 38 (1993) 2435.
[32] P.G.L. Baker, R.D. Sanderson, A.M. Crouch, Thin Solids Films 515 (2007) 6695.
[33] O. Chailapakul, E. Popa, H. Tai, B. Sarada, D. Tryk, A. Fujishima, Electrochem. Commun. 2 (2000) 422–426.
[34] S. Christoskova, M. Stoyanova, M. Georgioeva, Appl. Catal. A: Gen. 208 (2001) 243–249.
[35] P. Carnizares, M. Diaz, J.A. Dominquez, J. Garcia-Gomez, M.A. Rodrigo, Ind. Eng. Chem. Res. 41 (2002) 4187–4194.
[36] L. Zhao, H. Lee, J. Chromatogr. A 931 (2001) 95–105.
[37] O. Fiehn, M. Jekel, J. Chromatogr. A 769 (1997) 189–200.
[38] D. Gomis, N. Palomino, J. Alonso, Anal. Chim. Acta 426 (2001) 111–117.
[39] E. Fockedey, A. Van Lierde, Water Res. 36 (2002) 4169–4175.
[40] B. Bartolome, M. Bengoechea, M. Galvez, F. Perez-Ilzarbe, T. Hernandez, I. Estrella, C. Gomez-Cordoves, J. Chromatogr. A (1993) 119–125.
[41] C. Bock, B. MacDougall, J. Electrochem. Soc. 146 (8) (1999) 2925–2932.
[42] B. Korbarti, A. Tanyolac, Water Res. 37 (2003) 1505–1514.
[43] P. Wang, H. Lee, J. Chromatogr. A 789 (1997) 451–473.
[44] G. Shui, L. Leong, J. Chromatogr. A 977 (2002) 89–96.
[45] M. Castillo, D. Barcelo, Anal. Chim. Acta 426 (2001) 253–264.
[46] Y.J. Feng, X.Y. Li, Water Res. 37 (2003) 2399–2407.
[47] R. Portela Migklez, J. L6pez Bernal, E. Nebot Sanz, E. Martinez de la Ossa, Chem. Eng. J. 67 (1997) 115–121.
[48] C.-H. Chiou, et al. Chem. Eng. J. 139 (2008) 322–329.
[49] A. Quintanilla, J.A. Casas, A.F. Mohedano, J.J. Rodríguez, Appl. Catal. B: Environ. 67 (2006) 206–216.
[50] D. Duprez, J. Delanoë, J. Barbier Jr., P. Isnard, G. Blanchard, Catal. Today 29 (1996) 317.
[51] C. Bock, B. MacDougall, J. Electroanal. Chem. 491 (2000) 48–54.
[52] J. Hu, J. Zhang, C. Cao, Thermochim. Acta 71243 (2003) 1–10.
[53] V. Baglio, A. Di Blasi, T. Denaro, V. Antonucci, A.S. Aricò, R. Ornelas, F. Matteucci, G. Alonso, L. Morales, G. Orozco, L.G. Arriaga, J. New Mater. Electrochem. 11 (2) (2008) 105–108.